ORIGINAL PAPER

Composition and Structure of Human Gallstones Studied by Analytical TEM and EPR Spectroscopy

**V. V. Pantyushov[1] · O. M. Zhigalina[2,3] · D. N. Khmelenin[2] · I. A. Kokorin[4] ·
W. E. Trommer[5] · Y. N. Degtuarev[6] · A. I. Kokorin[6,7]**

Abstract

Using analytical transmission electron microscopy (TEM) in different variants, X-ray diffraction (XRD), elementary analyses, and *X*-band electron paramagnetic resonance (EPR) methods, the composition and structural peculiarities of human gallbladder stones (GSs) of various types removed during surgery from five patients with cholelithiasis were studied. TEM and EPR results showed heterogeneous composition and structure of GSs studied. These methods yield mutually complementary structural information. Characteristic EPR parameters of paramagnetic centers (PCs) have been determined as well as their nature and their average concentrations in the GSs samples were measured. In the case of iron ions, values of Fe^{3+} content measured by EPR and analytical TEM are in a good agreement. We believe that obtaining data on the structure and detailed composition of gallstones will allow prevention to be optimized in the future, and possibly will create new approaches to drug therapy of the cholelithiasis.

✉ W. E. Trommer
trommer@chemie.uni-kl.de

✉ A. I. Kokorin
alex-kokorin@yandex.ru; kokorin@chph.ras.ru

1   Pirogov City Clinical Hospital No. 1, Moscow, Russia

2   Shubnikov Institute of Crystallography, Federal Scientific Research Centre "Crystallography and Photonics", Russian Academy of Sciences, Moscow, Russia

3   Bauman State Technical University, Moscow, Russia

4   N. I. Pirogov Russian National Research Medical University, Moscow, Russia

5   Department of Chemistry, Technische Universität Kaiserslautern, P.O.Box 3049, 67653 Kaiserslautern, Germany

6   N. N. Semenov Federal Research Center for Chemical Physics, Russian Academy of Scieces, Moscow, Russia

7   Plekhanov Russian University of Economics, Moscow, Russia

1 Introduction

Cholelithiasis, the formation of gallstones (GSs) is one of the most common pathologies of the gastrointestinal tract [1–6]. Currently, a clear tendency to the increase of the disease frequency is observed on all population groups conditioned with growth of provoking factors presenting in the modern world [7–12]. Increasing life expectancy of the population and chronicity of many diseases which are a provoking factor themselves for the cholelithiasis development as well as dyshormonal concomitant disorders and presence in the diet of food rich with cholesterol and food additives lead to an increase of many diseases accompanied with a formation of pathological mineral particles in an organism [11–14].

Average incidence of cholelithiasis diseases doubles every decade and has a tendency to rejuvenation [11, 13]. Currently, the disease is detected in 10–20% of the total adult population. Every year in Russia are diagnosed up to 800,000 cases of the disease which need very complex surgery treatment and a long period of patient rehabilitation. Removal of the gallbladder with calculi is the most common abdominal surgery in the world. Number of complications after operations on the bile duct varies from 3.7 to 37.3% [15]. The number of cholelithiasis diseases will grow in the nearest future. In USA, treatment of gallstone disease and its complications costs up to five billion USD annually [8, 16].

Despite significant advantages in cholelithiasis surgery, steady increase in the incidence of the disease stimulates modern gastroenterology to prevention and treatment of the initial stages of the gallstone disease preventing the development of the process [4, 5, 7]. Therefore, the study of the etiology of the disease and pathogenesis of primary factors leading to GSs formation (agglomeration of various components of bile) becomes an important point in solving this problem.

Among modern hypotheses concerning factors forming gallstones, the most popular is an idea on the accumulation of peroxide products and free radicals in bile, which leads to destabilization of colloidal equilibrium, formation of crystals of cholesterol monohydrate and further precipitation of bile [1, 17–19]. For better understanding mechanisms, peculiarities of physical–chemical processes occurring during the development of gallstone disease, bile properties and details of composition and organization of GSs should be clarified.

Electron microscopy (EM) has widely been used in biological and medical investigations during many decades [20–22]. Currently, EM is one of the main tools of scientific and technical development of the research methods in medicine and biology, *e.g.*, for accurate diagnosis and histological analysis of biopsy materials, gallbladder calculi, etc. [23–28].

Analysis of advantages and disadvantages of visualizing components obtained by scanning electron microscopy (SEM) method is given in Ref. [29]. Usage of focused electron beams provided high resolution of 3*D* imaging for topographic morphology and detailing the surface of solid samples. Disadvantages of SEM are connected with high cost of the equipment and the necessity to place it in rooms completely isolated from electric and magnetic fields and also from possible vibrations [30]. Some peculiarities of the effect of polyethylene glycol-fibrin

gels on the cell migration has been described using SEM in combination with FT-IR, thermogravimetry analysis, atomic force microscopy and small-angle *X*-ray scattering (SAXS).

Articles [31–33] represent results obtained by the SEM method, in which examples of GSs extracted from different patients and varied by color, structure and chemical composition were studied. These papers have reported about significant heterogeneity of GSs by phase and elemental composition what the authors connected with various conditions of their occurrence and by different kinetics of their growth. The X-ray phase analysis (XRD) method showed [33] that except for two types of cholesterol and bilirubin in GSs, several modifications of $CaCO_3$ (valerite, calcite and aragonite) exist, and the energy dispersive spectra (EDS) revealed the presence of different chemical elements in various quantities: S, P, Fe, K, Na, etc. The calcites can also contain different metal ions including pointed out above and others.

Complex application of transmission electron microscopy (TEM) methods such as bright field (BF) and dark field (DF) images, electron diffraction (ED), scanning transmission electron microscopy (STEM) with z-contrast, obtaining maps of chemical elements distribution (EDX-mapping) with high locality open up new opportunities for detecting structural and chemical heterogeneities in GSs due to higher sensitivity and resolution comparing to scanning electron microscopy (SEM). They allow obtaining much more detailed information about changes in structure and chemical composition of the samples. A resolution in STEM EDX-mapping is mainly determined by a diameter of the probe (the electron beam) and can be reached up to 2–3 nm while the locality of EDX-mapping in SEM is about 1.0 um. It is known that sensitivity of electron diffraction phase analysis is sufficiently higher as compared to XRD, especially when combination of high resolution TEM images and Fourier diffraction patterns are additionally applied for structural investigations.

Electron paramagnetic resonance (EPR) spectroscopy provides a unique opportunity for studying medical and biological systems [34–39]. This is caused by (i) its high sensitivity, (ii) registration of only paramagnetic atoms, *i.e.,* radicals and certain ions in the sample, and (iii) possibility of selective identification of various paramagnetic centers (PCs). For example, in Ref. [35], application of the EPR technique is discussed in detail for registration of free radicals and metal ions in medicine and physiology including development perspectives for different problems which can be solved using EPR. The obtained results and an increasing role of EPR in application of stable spin labels and probes as a method of quantitative structural analysis along with nuclear magnetic resonance and *X*-ray diffraction method in studying biological membranes and membrane proteins have been discussed in the book [36].

A method of EPR microscopy (EPRM) with submicron resolution (~700 nm) at high concentration of spins in the sample has been suggested [38]. Some advantages of EPRM in biomedical research were demonstrated with rat basophilic leukemia cells and on samples of cancerous tissues with a resolution of several microns using water-soluble trityl spin probes. EPRM can be also applied for studying mobility and cell metabolism in various conditions of cell growth.

We should note that the EPR method has already found a fairly wide application in clinical studies of internal diseases [34, 40] including cholelithiasis and elucidation of the mechanisms of formation of gallstones as well [41–43, 43]. As an example, the study of mixed cholesterol GSs showed that free radical distribution is heterogeneous inside GSs [41]. Morphological type and amount of PCs depend on pigment content in the selected sample fragment. EPR parameters of some pigments have been measured. It is important that authors of these papers have observed and characterized several PCs, *e.g.*, stable free bilirubin radical (BLR), manganese, iron and copper ions, they tried to estimate their content in GSs. Details of these works we will consider below in the relevant section under discussing our own results.

These cited articles published by several research groups, unfortunately, were fragmentary and not correlated with each other, and were carried out on gallstones of different types, which produced difficulties in comparing the results obtained in them. In this paper, we present the first results obtained using TEM and EPR technique of systematic investigation of the structure, spatial distribution and spectral properties of gallstones isolated during surgery from patients with cholelithiasis of various etiology.

2 Experimental

In this work we studied gallstones (GSs) extracted from five patients during cholelithiasis operations, which are shown in Fig. 1. Samples were chosen based on different morphology and chemical composition.

2.1 Description of GSs Morphology

Figure 1 represents photos of GSs samples chosen for the analysis. Morphological description of the samples is given below. All GSs samples were obtained during laparoscopic cholecystectomy in a planned manner. After seizure, samples were dried at room temperature and stored in sterile Eppendorf tubes.

Sample N1: GSs of yellow color, multiple, polyhedral with rounded edges; size of 0.4–0.7 cm, with a smooth, shiny surface, dense, with layered structure. From macroscopic view, it was assumed that these GSs are of cholesterol type.

Sample N2: Brown pigmented (fulvous) calculi, multiple, hexagonal with rounded edges; size of 0.5–0.6 cm, with a smooth, shiny surface, crumbling, soft.

Fig. 1 Gallstones used in this work. The sample N5 is packed in the plastic envelope with bile

Sample N3: One stone with deep brown color, irregular oval shape; size 1.0–1.3 cm with a smooth mat surface, soft, crumbly, layered. GSs are of a mixed (cholesterol-pigment) composition with a predominance of the cholesterol component.

Sample N4: multiple calculi of multifaceted irregular shape with sharp edges are of size 0.2–0.8 cm, brown color with a greenish tint, a smooth, shiny surface, dense, layered. GSs are of a mixed composition with a predominance of the cholesterol-bilirubin component.

Sample N5 is a single calculus, large, size 1.8 cm, of irregular multifaceted shape with sharp edges, black with light blotches, with a rough surface, fragile, crumbling into small lamellar crystals.

Samples of gallstones were ground in a porcelain mortar, placed in test tubes with acetone and dispersed in an ultrasonic bath, then, droplets of suspension were put to special copper grids with a thin amorphous lacey carbon film for further study in a microscope. The following methods were applied for structural investigation: transmission electron microscopy (TEM), scanning transmission electron microscopy (STEM) with a high angle angular dark field detector (HAADF), electron diffraction, energy dispersive X-ray analysis (EDX) in a FEI Tecnai Osiris microscope. The microscope is equipped with a silicon detector system SuperX (Bruker) for ultra-fast elemental mapping at accelerating voltage of 200 kV.

Samples for EPR spectroscopy were prepared in two ways: (*a*) a gallstone was cut with a ceramic knife to small parts, *c.a.*, $2 \times 2 \times 2$ mm, choosing for further measurements particles with similar color or (*b*) rubbing GSs in a porcelain mortar to particles with a diameter of *ca*. 0.2–0.3 mm. Then, GSs material was placed into thin-walled quartz ampoules (3.5–4.0 mm in diameter). Measurements were carried out in the presence of air without pumping. EPR spectra were recorded on CW *X*-band Bruker EMX-8 spectrometer at 298 and 77 K in the Center of Magnetic Spectroscopy at N. M. Emanuel Institute of Biochemical Physics, Russian Academy of Sciences. For measurements, a microwave frequency of 9.65 GHz, a modulation frequency of 100 kHz; and microwave power of 0.2 mW was used. The relative and absolute contents of paramagnetic centers, PCs, in the samples were evaluated by double integration of the spectra and by comparison of the results with a reference, the spectrum of a $CuCl_2 \cdot 2H_2O$ single crystal with a known number of spins. Analysis of experimental EPR spectra was carried out with the use of the software package "Simulation of rigid limit and slow motion EPR spectra" provided by Prof. A. Kh.Vorobyev, Faculty of Chemistry, M. V. Lomonosov Moscow State University.

3 Results and Discussion

3.1 TEM Results

Figure 2 demonstrates HAADF STEM images of fragments of sample N2 which show particles differing in structure: porous (*a*), with fibrous structure (*b*), and polycrystalline with round-shape crystals with sizes up to 0.3 μm (*c*).
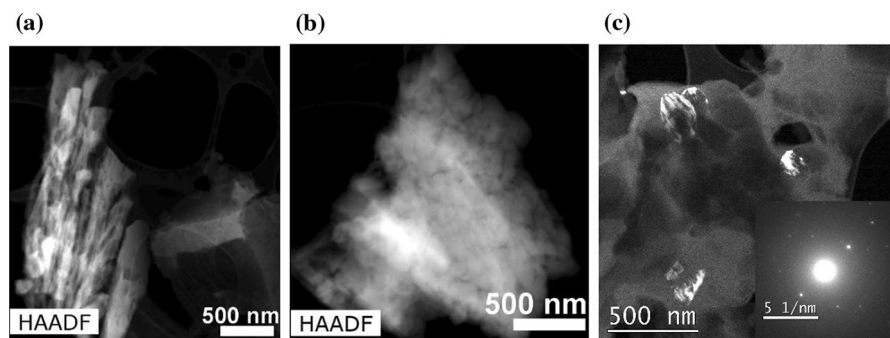
Fig. 2 HAADF STEM images of porous (**a**) and fibrous (**b**) fragments, and a DF image (**c**) with a corresponding selected area diffraction (SAED) pattern taken from crystals of the sample N2
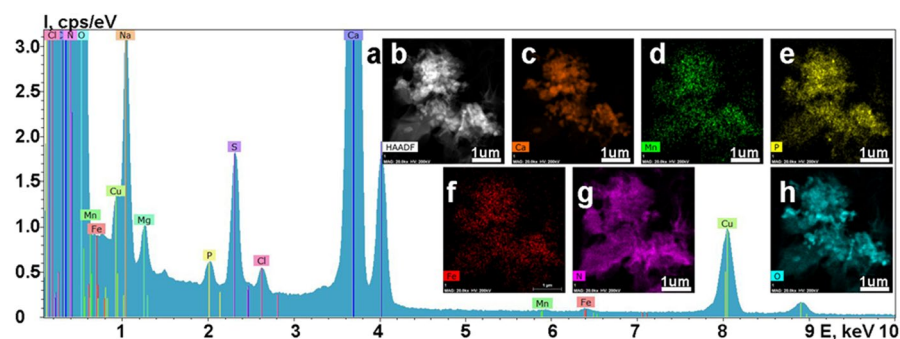

Fig. 3 EDX-spectrum (**a**), HAADF STEM image (**b**), and corresponding distribution maps of chemical elements (**c–h**) of this area for sample N2

EDX spectra of N1 and N2 particles showed that peaks corresponding to iron were absent. Analysis of SAED patterns and comparing with maps of chemical element distribution (Fig. 3) showed that particles of the round shape are $CaCO_3$ in valerite and aragonite modifications which are the main phases characteristic of this sample. Besides, a peculiarity of the elementary composition of such particles is the high content of sulfur and phosphorus following from the height of corresponding peaks in the spectrum (Fig. 3), Mg, Al, K are also observed. Iron is present in small amounts, however, not in every spectrum. In the areas where the iron peak is clearly seen in a spectrum of N2 (Fig. 3f), its distribution differs from sample N1 by homogeneous, random distribution in the sample, and not in separated tiny particles as in N1 (Fig. 3).

From the results of quantitative analysis given in Table 1 one can see that iron and manganese are distributed heterogeneously in the investigated samples (Fig. 4).

Analysis of TEM and STEM patterns together with elementary analysis data of GSs N1 showed that particles have arbitrary shapes, and the EDX-spectrum has revealed the essential elements in the sample: Ca, O, Na, as well as S, P, Cl in

Table 1 The relative content of the elements (*K*-series) in samples N1–N5

Sample	Element	[wt.%]	[at.%]	Error, wt.%
	Calcium	98.10	98.62371	10.58
N1	Manganese	0.87	0.634544	0.66
	Iron	1.03	0.741744	0.72
Total		100	100	
	Calcium	84.57	88.42	57.32
N1*	Manganese	0	0	0
	Iron	15.43	11.58	6.83
Total		100	100	
	Calcium	99.45	99.60	9.03
N2	Manganese	0.19	0.14	0.10
	Iron	0.36	0.26	0.11
Total		100	100	
	Calcium	98.7	99.06	9.14
N3	Manganese	0	0	0
	Iron	1.30	0.94	0.33
Total		100	100	
	Calcium	98.99	99.26	9.02
N4	Manganese	0.83	0.61	0.18
	Iron	0.18	0.13	0.12
Total		100	100	
	Calcium	97.53	98.21	9.19
N5	Manganese	0.09	0.06	0.05
	Iron	2.34	1.723842	0.55
Total		100	100	

*The relative content of elements in the particle area containing Fe in Fig. 3
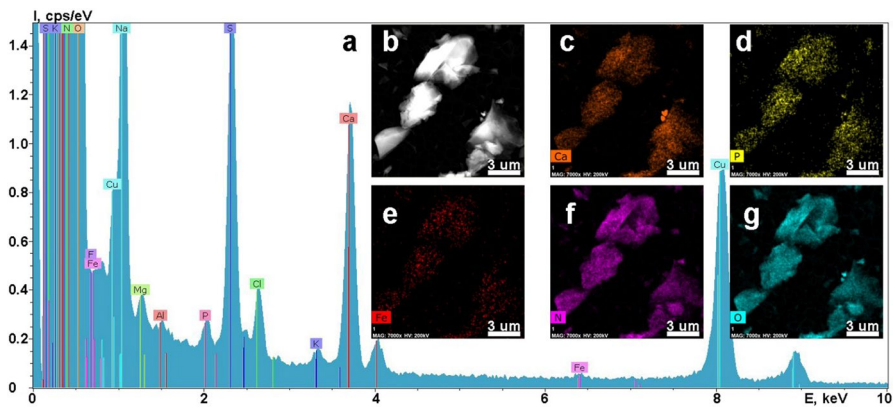
Fig. 4 EDX-spectrum (**a**), HAADF STEM image (**b**), and corresponding EDX-mapping (**c–g**) of this area for sample N5

smaller amounts. Iron ions were revealed only in a few maps as one-two inclusions with a rounded shape and the size of 0.3 μm. The inclusions contained Fe and P simultaneously, and their distributions were identical. The same areas contained also sodium ions. Except for iron and phosphorus, the rest elements are distributed in the particles homogeneously. The data of relative contents of iron, manganese and calcium in the samples are listed in Table 1. For getting a general picture, we have analyzed several maps of each sample.

A characteristic peculiarity of the particles content in sample N3 is the increased quantity of Na, S, P, while it contains considerably less Ca as compared to samples N1 and N2. The rest elements are present in similar amounts as in other samples. Also, in small amounts, there are Mg, Al, Cl, K. Manganese peaks are not observed in EDX spectra. A distribution of all elements is homogeneous throughout the whole surface area of all N3 particles studied.

In sample N4, we have revealed the increased content of Mn and of phosphorus which as well as Ca and O are the main elements in these particles. Such elements as Na, Mg, Al, Cl, K, S were observed in much smaller amounts, and Fe was detected as traces. Comparing distribution maps of the elements, one can assume that particles of N4 sample contain primarily compounds of Ca, Na, P, O, there are also substances of sodium with sulfur.

High content of sulfur has been found in sample N5 while peaks of other elements (Mg, Al, Cl, F) were approximately the same as in other samples. Traces of Fe were also observed in the EDX spectrum, which was distributed homogeneously in the volume of the particles.

EDX-mapping investigation showed that iron is usually present but not in all areas of the sample and differs by its distribution: homogeneously in the whole volume of a map or inhomogeneously in the content of some small particles with sizes of a part of a micron. The elemental composition is characterized by calcium, oxygen, carbon as well as sodium, sulfur, phosphorus and nitrogen. Some metals are also revealed: magnesium, manganese, potassium, iron. Compounds which contain metals can be visualized much easier by EDX-mapping. Presence of bilirubin ($C_{33}H_{36}N_4O_6$) in the samples follows indirectly from the fact that the elemental distribution maps of nitrogen and oxygen are identical. But the presence of cholesterol ($C_{27}H_{46}O$) cannot be detected by EDX-mapping due to the carbon substrate usage and impossibility of registering hydrogen atoms with the EDX detector.

We could conclude from the experimental results that there is a crystalline phase of $CaCO_3$ with different morphology in all five samples of gallstones. These calcites can include various metals: K, Al, Mg, Mn, etc. Our data indicate formation of minerals with different composition as well as sulfides, metal compounds inclusions and bilirubin. Our results qualitatively agree well with the data published in literature [28, 33, 44].

3.2 EPR Results

Recording of EPR spectra of all samples N1-N5 has initially been carried out at room temperature with conditions approximately close to natural. As an example,
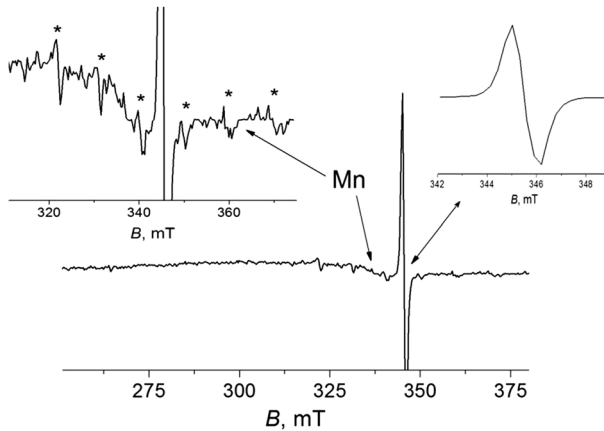
Fig. 5 EPR spectra of sample N2 at 298 K. Left insert: enlarged central part of the spectrum. Right insert: spectrum of free radicals. Stars denote EPR lines of manganese ions

Fig. 5 presents a spectrum of sample N2 at 298 K which clearly shows existence of at least two EPR signals with different paramagnetic centers (PCs) in N2—a stable organic radical and manganese ions illustrated by six main lines in the EPR spectrum. Low signal-to-noise ratio at 298 K does not allow correct identification of the type and valence of manganese ions. The intensive radical signal with a g-factor value of *ca*. 2.003 and a line width $\Delta B \approx 1.0$ mT is typical to GSs of the cholesterol type, and the unpaired electron is localized on the bilirubin molecule [41–43].

Similarly to the previous figure, the EPR spectrum of sample N5 points to the presence in this GSs of not less than three types of PCs (Fig. 6): (i) the signal of bilirubin padical R, (ii) iron ions Fe^{3+} and, most likely, (iii) ions of copper(II).
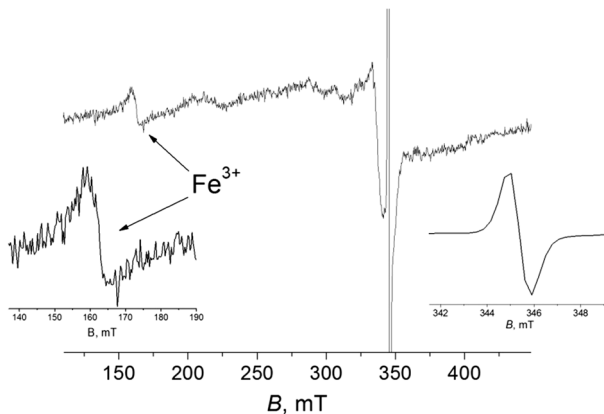

Fig. 6 EPR spectra of sample N5 at 298 K. Left insert: enlarged spectrum of iron ions. Right insert: enlarged spectrum of free radical
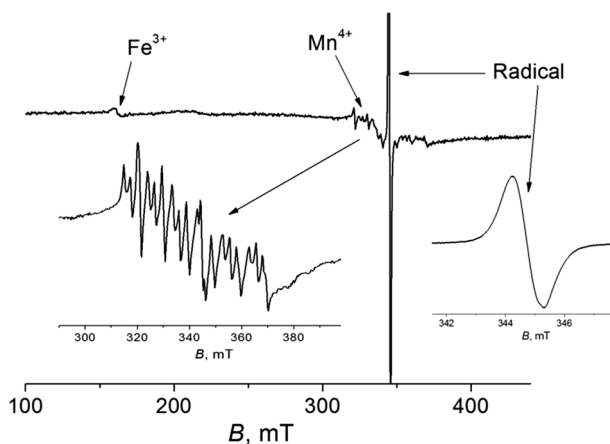
Fig. 7 EPR spectra of sample N2 at 77 K. Left insert: enlarged central part of the spectrum. Right insert: enlarged spectrum of free radicals
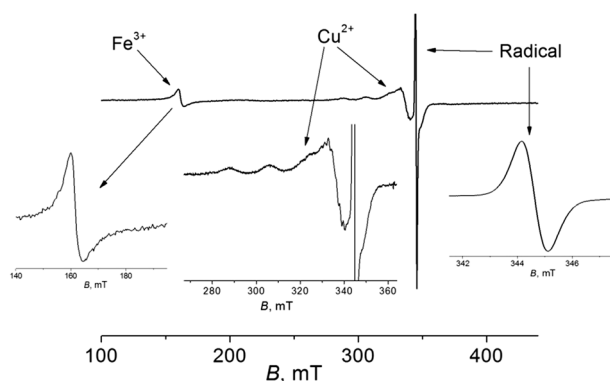

Fig. 8 EPR spectra of sample N5 at 77 K. Left insert: enlarged spectrum of iron ions. Central insert: enlarged spectrum of copper(II) ions. Right insert: enlarged spectrum of free radicals

For the exact identification of PCs, we have recorded EPR spectra of these samples at 77 K as well which are shown in Figs. 7, 8.

Recording the EPR spectra at lower temperature leads to stopping molecular movements, to elongation of the spin–lattice relaxation time of PCs, i.e., to the decrease of EPR line widths and as a result to increasing signal-to-noise ratio and to increasing the sensitivity of the EPR spectrometer. For example, it was revealed for sample N2 (Fig. 7) that besides the radical R of manganese ions registered at 298 K, there is also some amount of Fe^{3+} ions which had not been observed at room temperature. The EPR spectrum of manganese in Fig. 7 indicates its presence in the gallstone. Firstly, there are not only Mn^{2+} ions containing five unpaired electrons (electron spin $S = 5/2$) and nuclear spin $I = 5/2$ with a lot of transitions between the spin states, but also probably Mn^{4+} ions what significantly complicates their

quantitative analysis. Secondly, from the spectral shape shown in the left insert follows that a certain portion of manganese ions is distributed in the GSs volume as isolated magnetically diluted PCs while some portion of ions participate in magnetically concentrated aggregates in which ions are coupled by strong spin–spin interaction [46].

In the case of sample N5, analysis of EPR spectra at 77 K confirmed the presence of three types of PCs and showed unequivocally that the central EPR signal relates to the isolated Cu^{2+} complexes (Fig. 8), which was not evident from the spectrum at 298 K (Fig. 6). In EPR spectra of samples N2 and N5 recorded at 77 K, instrumental noise is practically absent and thus significantly improving the analysis of the composition and structural peculiarities of the samples. A similar effect of increasing the sensitivity we have also observed in the case of the rest samples.

Analysis of EPR spectra of all samples investigated has demonstrated that the nature and composition of paramagnetic centers in them are sufficiently different, and in some cases even inside a certain gallstone. For example, all N1–N5 samples contain free radicals R which are stabilized in the bilirubin molecule [41–43] but in various concentrations (Table 2). In four samples (N2–N5) iron Fe^{3+} ions were revealed, in N2—manganese ions, and in N3 and N5—coordinated copper Cu^{2+} ions. EPR parameters of R and Fe^{3+} ions are given in Table 2. A measured value of $g^{Mn} = 2.001 \pm 0.001$ is typical for ions both of Mn^{2+} and Mn^{4+} PCs [45–47]. A very weak manganese signal has also been observed in sample N4. Some variation of g^R and ΔH^R values for radicals R and of their line shape in different samples indicate either the existence of several radical types present in various concentrations or on differences in their local (neighboring) environment (polar groups or counter-ions).

We should note that Mössbauer and EPR spectra of pigment gallstones recorded at room temperature indicated the existence of iron in the high-spin Fe^{3+} state of low symmetry with a $g = 4.28$ signal. Elemental analysis showed the presence of Cu, Mn, Zn, and Pb except iron [48].

Values determined in this work agree well with those reported in literature, *e.g.*, with $g^R = 2.0032$, $g^{Fe} = 4.19$ [41], $g^R = 2.003$, $\Delta H = 1.0$ mT and $g^{Fe} = 4.19$ [43] corresponding to the bilirubin radicals and Fe^{3+} ions.

The EPR spectra of divalent copper Cu^{2+} ions in sample N5 and the much weaker one in sample N3 have the following parameters: $A_{\parallel}^{Cu} = 184 \pm 4$ G, $g_{\parallel}^{Cu} = 2.191 \pm 0.005$; $g_{\perp}^{Cu} = 2.051 \pm 0.004$, and $a_{\perp}^{N} = 13.9 \pm 0.2$ G, where $A_{\parallel}^{Cu}$ is a hyperfine splitting (hfs) constant, and $g_{\parallel}^{Cu}$ and $g_{\perp}^{Cu}$ are the main values of the g-tensor characterizing Zeeman spin-orbital interaction. The spectral shape (Fig. 8)

Table 2 EPR parameters, g-factors of paramagnetic centers (g^R) and Fe^{3+} (g^{Fe}) in gallstones			
Sample	$g^R \pm 0.0005$	$\Delta H^R \pm 0.2$ G	$g^{Fe} \pm 0.01$
N1	2.0038	10.7	–
N2	2.0037	10.4	4.27
N3	2.0039	10.5	–
N4	2.0034	9.9	4.28
N5	2.0038	9.8	4.27

and the measured values of $A_\parallel^{Cu}$, $g_\parallel^{Cu}$, and $g_\perp^{Cu}$ indicate that copper ions exist in the form of isolated mononuclear complexes with four nitrogen atoms (^{14} N) in the coordination sphere [47–49]. A value of the super-hyperfine splitting constant $a_\perp^N$, equal to 13.9 G, is characteristic for the octahedral structure of the Cu^{2+} complex with four ^{14} N atoms in the equatorial plane [49–51]. Whereas acid residues and low molecular complexones forming the Cu(II) coordination sphere are not defined yet although we can definitely say from measured parameters of $g_\parallel$ and $A_\parallel$ that these are nitrogen-coordinating amino acid groups of histidine, lysine, and possibly ornithine [47, 51]. Similar parameters were determined, *e.g.*, for a signal, with $g_\perp = 2.05$ and $g_\parallel = 2.20$, published in [41] while in Refs. [42, 43] were estimated such values as $g_\perp = 2.05$, $g_\parallel = 2.37$, $A_\parallel = 18.6$ mT. This indicates a possibility of also existing COO^- groups of organic or amino acids it the coordination sphere of copper ions.

We have applied a double integration method to recorded EPR spectra in the cases when the signal-to-noise ratio was reasonable according to recommendations of Ref. [52] and we have determined concentrations of PCs in the samples which are listed in Table 3. The content of manganese ions could not be determined by the integration of EPR spectra due to its complex shape and the superposition of several signals in this region of the N2 GSs EPR spectrum. Results are given in Table 3 where they are compared with the data of the electron microscopy analysis.

3.3 Discussion

The results obtained confirm earlier conclusions about the composition of gallstones in which in a very wide range of concentrations of organic compounds as cholesterol, bilirubin, proteins, bile and other organic acids) as well as inorganic ions, salts, and complexes of alkaline earth (Ca, Mg), alkaline (Na, K), and transition metals (Fe, Mn, Cu, Zn, Al), and also compounds of non-metals (C, O, N, P, S, Cl) are pesent. Variety of composition and structure of GSs requires researchers to apply different physical and spectroscopic methods to obtain reliable information.

In this work we have examined a group of five gallstones of different morphology with the use of transmission electron microscopy (TEM) and electron paramagnetic resonance (EPR). Results obtained (see Table 3) demonstrate the complementarity of these methods. Indeed, TEM can measure the content of diamagnetic ions such as

Table 3 Content of various elements in gallstones from EDX and EPR data

Sample	Transmission electron spectroscopy			Content of [PCs] $\times 10^{-16}$, spin/g		
	Ca, %	Mn, %	Fe, %	Fe^{3+}	Cu^{2+}	Radical
N1	98.1 ± 10.6	0.87 ± 0.66	1.03 ± 0.72	–	–	0.9 ± 0.4
N2	99.4 ± 9.1	0.11 ± 0.09	0.21 ± 0.11	1.3 ± 0.2	–	5 ± 0.6
N3	98.7 ± 9.1	0	1.30 ± 0.33	3.9 ± 0.3	51 ± 10	1.1 ± 0.5
N4	99.0 ± 9.0	0.83 ± 0.18	0.18 ± 0.11	2.1 ± 0.2		7 ± 1
N5	97.2 ± 9.2	0.19 ± 0.15	2.61 ± 0.52	8.5 ± 0.7	290 ± 30	11.5 ± 1

calcium, not detected by EPR which detects with high precision paramagnetic ions of Fe^{3+}, Cu^{2+} as well as bilirubin radicals R in the samples.

4 Conclusion

Studies of the composition and structural peculiarities of human gallbladder stones (GSs) of various types removed during surgery operations from five patients with cholelithiasis using analytical transmission electron microscopy (TEM) and electron paramagnetic resonance (EPR) methods showed heterogeneous content and organization of GSs studied. EPR and analytical TEM are mutually complementary by obtaining information about gallstones. Characteristic EPR parameters of paramagnetic centers (PCs) have been determined as well as their nature and their average concentrations in the GSs samples. Analytical TEM gave a unique information about diamagnetic components and phase structure of GSs. Copper(II) complexes were evidently observed and characterized. Good agreement between data determined by TEM and EPR in the case of Fe^{3+} ions contained in all samples studied permits to hope that further joint application of these two methods will provide valuable information for the therapy of cholelithiasis. In the case of gallstones, such mutual application of these two methods is realized for the first time.

Although currently there are no direct potential medical implications or benefits from quantitative knowledge of the composition of the gallstones (GSs) and their heterogeneity, one should take into consideration that the correct therapeutic treatment of the cholelithiasis could be suggested only by understanding the mechanism of the disease, its etiology and pathogenesis, therefore, detailed information about the precise structural features of gallstones is quite necessary. Different physical methods provide various and rather often contradictory results which have to be additionally checked using other methods. Such methods as analytical TEM and EPR allow obtaining complementary data about atoms, ions and species contained in GSs and their comparison with the disease history may provide such valuable therapeutic information.

References

1. YuKh. Marahovskii, J. Gastroenterol. Hepatol. Coloproctol. **13**, 81 (2003)
2. M.Y. Berger, J.J. van der Velden, J.G. Lijmer, H. de Kort, A. Prins, A.M. Bohnen, Scand. J. Gastroenterol. **35**, 70 (2000)
3. H.-U. Marschall, C. Einarsson, J. Int. Med. **261**, 529 (2007)
4. V.P. Gatsenko, E.R. At'kova, R.A. Ivanchenkova, Treating doctor, No. 7, 15 (2011)
5. T.E. Skvortsova, S.I. Sitkin, V.G. Radchenko, P.V. Seliverstov, E.I. Tkachenko, Gallstone disease. Current approaches to to diagnosis, treatment and prevention (Forte Print, Moscow, 2013) (in Russian)
6. A. Nakeeb, A.G. Comuzzie, L. Martin, G.E. Sonnenberg, D. Swartz-Basile, A.H. Kissebah, H.A. Pitt, Ann. Surg. **235**, 842 (2002)
7. E.I. Vovk, Consilium medicum. Gastroenterology **2**, 4 (2010)
8. J.E. Everhart, M. Khare, M. Hill, K.R. Maurer, Gastroenterology **117**, 632 (1999)
9. S. Abraham, H.G. Rivero, I.V. Erlikh, L.F. Griffith, V.K. Kondamudi, Am. Fam. Phys. **89**, 795 (2014)
10. I.N. Grigor'eva, S.K.K. Malyutina, M.I. Voevoda, Exper. Clin. Gastroenterol. **4**, 64 (2010)
11. H. Sun, H. Tang, S. Jiang, L. Zeng, E.-Q. Chen, T.-Y. Zhou, Y.-J. Wang, World J. Gastroenterol. **15**, 1886 (2009)
12. N. Mendez-Sanchez, J. Bahena-Aponte, N.C. Chavez-Tapia, D. Motola-Kuba, K. Sánchez-Lara, G. Ponciano-Radríguez, M.H. Ramos, M. Uribe, Am. J. Gastroenterol. **100**, 827 (2005)
13. C.F. Chen, M.S. Kong, M.W. Lai, C.J. Wang, Acta Paediatr. Taiwan **47**, 192 (2006)
14. T. Berhane, M. Vetrhus, T. Hausken, S. Olafsson, K. Søndenaa, Scand. J. Gastroenterol. **41**, 93 (2006)
15. V.V. Rodionov, M.I. Filimonov, V.M. Moguchev, Calculous cholecystitis complicated with obstructive jaundice (Medicine, Moscow, 1991) (in Russian)
16. A.A. Prizentsov, V.M. Lobankov, A.G. Skuratov, Probl. Health Ecol. **3**(33), 39 (2012)
17. C.L. Hawkins, M.J. Davies, Biochim. Biophys. Acta **1840**, 708 (2013)
18. M. Valko, D. Leibfritz, J. Moncol, M.T. Cronin, M. Mazur, J. Telser, Int. J. Biochem. Cell Biol. **39**, 44 (2007)
19. M. Valko, C.J. Rhodes, J. Moncol, M. Izakovic, M. Mazur, Chem. Biol. Interact. **160**, 1 (2006)
20. J.C.H. Spence, *Experimental High-Resolution Electron Microscopy* (Clarendon Press, Oxford, 1988)
21. Y.Y. Komissarchik, A.A. Mironov, *Electron Microscopy of Cells and Tissues* (Nauka, Leningrad, 1990)
22. A.A. Mironov, Y.Y. Komissarchik, V.A. Mironov, *Methods of Electron Microscopy in Biology and Medicine* (Nauka, St. Peterburg, 1994)
23. J. Thomas, T. Gemming, *Analytical Transmission Electron Microscopy* (Springer, Dordrecht, 2013)
24. G. Macchiarelli, M. Motta, T. Fujita, Scanning electron microscopy of the liver cells, in *Biopathology of the Liver*. ed. by P.M. Motta (Springer, Dordrecht, 1988), pp. 37–57
25. E.R. Fischer, B.T. Hansen, V. Nair, F.H. Hoyt, D.W. Dorward, *Scanning Electron Microscopy*, 2nd edn. (John Wiley, New York, 2012)
26. O.V. Volkova, V.A. Shakhlamov, A.A. Mironov, Atlas of scanning electron microscopyof cells, tissues and organs (Medicine, Moscow, 1987) (in Russian)
27. S. Thiberge, A. Nechushtan, D. Sprinzak, O. Gileadi, V. Behar, O. Zik, Y. Chowers, S. Michaeli, J. Schlessinger, E. Moses, Proc. Nat. Acad. Sci. USA **101**, 3346 (2004)
28. O.M. Zhigalina, D.N. Khmelenin, V.V. Labis, E.A. Bazikyan, S.V. Sizova, S.V. Khaidukov, V.E. Asadchikov, A.V. Buzmakov, Yu.S. Krivonosov, D.A. Zolotov, I.G. Kozlov, Crystallogr. Rep. **64**, 798 (2019)
29. O.P. Choudhary, C. Priyanka, Int. J. Curr. Microbiol. Appl. Sci. **6**, 1877 (2017)
30. A.I. Shpichka, P.V. Konarev, Yu.M. Efremov, A.E. Kryukova, N.A. Aksenova, S.L. Kotova, A.A. Frolova, N.V. Kosheleva, O.M. Zhigalina, V.I. Yusupov, D.N. Khmelenin, A. Koroleva, V.V. Volkov, V.E. Asadchikov, P.S. Timashev, RSC Adv. **10**, 4190 (2020)
31. G.G. Ustinov, V.V. Polyakov, Izv. Altai State Univ. **1**(89), 79 (2016). (**In Russian**)
32. S.S. Matrenin, A.A. Tishkin (2016) Izv. Altai State Univ. pp. 220–228

33. V.E. Asadchikov, A.V. Buzmakov, A.E. Voloshin, I.G. Dyachkova, O.M. Zhigalina, V.G. Basu, D.N. Khmelenin, D.A. Zolotov, A.G. Ivanova, Yu.S. Krivonosov, V.V. Pantyushov, R.G. Saifutdinov, Exper. Clin. Gastroenterol. **155**, 118 (2018)

34. R.G. Saifutdinov, L.I. Larina, T.I. Vakul'skaya, M.G. Voronkov, *Electron Paramagnetic Resonance in Biochemistry and Medicine* (Kluver Acad./ Plenum Publ., New York, 1993)

35. S.S. Eaton, G.R. Eaton, L.J. Berliner (eds.), *Biomedical EPR. Part A: Free Radicals, Metals, Medicine and Physiology* (Springer, Boston, 2005)

36. M.A. Hemminga, L. Berliner, *ESR Spectroscopy in Membrane Biophysics. Biological Magnetic Resonance* (Kluwer Acad./ Plenum Publ., New York, 2007)

37. G.I. Likhtenshtein, J. Yamauchi, S. Nakatsuji, A. Smirnov, R. Tamura, *Nitroxides: Application in Chemistry, Biomedicine, and Materials Science* (Wiley-VCH, Weinhem, 2008)

38. C.S. Shin, C.R. Dunnam, P.P. Borbat, B. Dzikovski, E.D. Barth, H.J. Halpern, J.H. Freed, Nanosci. Nanotechnol. Lett. **3**, 561 (2011)

39. V.V. Khramtsov, Antiox. Redox Signal. **28**, 1365 (2018)

40. L.B. Dudnik, N.G. Khrapova, Membr. Cell Biol. **12**, 233 (1998)

41. S.A. Kiselev, L.V. Tsyro, D.A. Afanasiev, F.G. Unger, M.M. Soloviev, J. Appl. Spectr. **81**, 141 (2014)

42. H.T. Sanikidze, M. Shengelia, E. Chikvaidze, S. Kiparoidze, N. Gogebashvili, P. Kuppusamy, Curr. Top. Biophys. **37**, 1 (2014)

43. H.T. Sanikidze, E. Chikvaidze, Radiat. Prot. Dosim. 1–8 (2016). https://doi.org/10.1093/rpd/ncw237

44. A. Pichugina, L. Tsyro, F. Unger, AIP Conf. Proc. **1899**, 050008 (2017). https://doi.org/10.1063/1.5009871

45. Y.S. Krivonosov, V.E. Asadchikov, A.V. Buzmakov, A.G. Ivanova, V.V. Artemov, A.A. Rusakov, V.V. Pantyushov, R.G. Saifutdinov, N.V. Minaev, S.A. Minaeva, M.A. Syachina, V.K. Popov, Crystallogr. Rep. **64**, 920 (2019)

46. Y.N. Molin, K.M. Salikhov, K.I. Zamaraev, *Spin Exchange* (Springer, Berlin, 1980)

47. S.A. Al'tshuler, B.M. Kozyrev, *Electron Paramagnetic Resonance (English Translation Ed. by CP Poole Jr.)* (Academic Press, New York, 1964)

48. H.A. Kuska, M.T. Rogers, *ESR of First Row Transition Metal Complex Ions* (Interscience, New York, 1968). (**Mir, Moscow, 1970**)

49. V.V. Saraev, F.K. Shmidt, *Electron Paramagnetic Resonance of Metal-Complex Catalysts* (Irkutsk State Univ. Publ, Irkutsk, 1985). (**in Russian**)

50. W. Chua-Anusorn, T.G. St. Pierre, J. Webb, K. Wang, J.F. Lu, Hyperfine Interact. **91**, 911 (1994)

51. A.I. Kokorin, The structure of coordination compounds with macromolecular ligands, Dr. Sci. Thesis, ICP RAS, Moscow, 1992

52. G.R. Eaton, S.S. Eaton, D.P. Barr, R.T. Weber, *Quantitative EPR* (Springer, Wien, 2010)